Fusion Engineering and Design 124 (2017) 306–310

Contents lists available at ScienceDirect

Fusion Engineering and Design

journal homepage: www.elsevier.com/locate/fusengdes

Thermal performance augmentation by rib-arrays for helium-gas cooled First Wall applications

Sebastian Ruck*, Benedikt Kaiser, Frederik Arbeiter

Karlsruhe Institute of Technology, Institute of Neutron Physics and Reactor Technology, Hermann-von-Helmholtz-Platz 1, 76344 Eggenstein-Leopoldshafen, Germany

HIGHLIGHTS

- V-shape rib-arrays are more efficient than comparable smooth channel flows.
- Heat transfer is significantly increase for channels structured by V-shaped rib-arrays.
- Thermal performance is significant increased by the investigated rib-arrays.
- Structured heat transfer surfaces provide an efficient cooling for the First Wall.

ARTICLE INFO

Article history:
Received 29 September 2016
Received in revised form 24 March 2017
Accepted 31 March 2017
Available online 19 April 2017

Keywords:
First wall cooling
Helium gas
Structured cooling channels
Rib-arrays
Detached eddy simulation

ABSTRACT

Rib-roughening the helium-gas cooling channels in the plasma facing components of DEMO (First Wall, limiters or the divertor) enhances heat transfer and reduces structural material temperatures. In the present study the applicability of six different surface-attached rib-arrays and of two different detached rib-arrays was examined for increasing the thermal performance within the helium-gas First Wall cooling concept. The rib-arrays consisted of transversally oriented or upstream directed 60° (with respect to the centerline) V-shaped ribs with different rib cross section (square, trapezoid, 2 mm radius round-edged front- and rear-rib-surface). Turbulent flow and heat transfer for 8 MPa pressurized helium-gas with a helium mass flow rate of 0.049 kg/s were computed by the Detached-Eddy-Simulation approach. A constant heat flux density of 0.75 MW/m^2 and 0.08 MW/m^2 was applied at the plasma-facing and breeding-blanket-facing First Wall structural surface respectively. The results showed that structuring the thermally highly loaded cooling channel surface with rib-arrays of 60° V-shaped ribs provides an efficient heat transfer and increases the cooling performance of the First Wall. The corresponding heat transfer coefficient was in the range from 7.1 to 7.5 kW/m^2 K and from 7.6 to 8.1 kW/m^2 K for the attached and detached V-shaped ribs respectively. Compared to smooth channel flows, only 14–16% of the pumping power is required to obtain an equivalent heat transfer performance or, from another point of view, the heat transfer coefficient can be increased by 168–172% for a constant pumping power.

1. Introduction

Pressurized helium-gas is a coolant in several breeding blanket (BB) design concepts of the envisaged DEMO fusion power reactor. Compared to water and liquid metals, helium is inert for chemical and nuclear reactions, causes no corrosion or activation and offers a wide temperature range for cooling without phase transformation. Improved designs of the First Wall (FW) cooling channels (CC) with rib-roughened or structured CC surfaces enhance the heat transfer and can compensate the comparable low volumetric heat capacity and thermal conductivity of helium-gas. The ribs placed at the thermally highly loaded CC surface induce a three-dimensional, unsteady flow field and heat transfer is augmented by mixing the fluid in the near wall regions and boundary layers providing a reduction of the maximum FW structural temperature [1]. It increases the functionality of the FW cooling performance and can raise the degree of efficiency of the primary heat transfer system and of the balance of plant. On the other hand, the ribs increase the flow resistance, and thus, the pumping power is raised (for unchanged mass flow rate) [2]. Furthermore, the manufacturing of rib-roughened CC surfaces is complex. However, the disadvantages due to increased flow resistance and complex manufacturing can

* Corresponding author.
E-mail address: sebastian.ruck@kit.edu (S. Ruck).

http://dx.doi.org/10.1016/j.fusengdes.2017.03.171

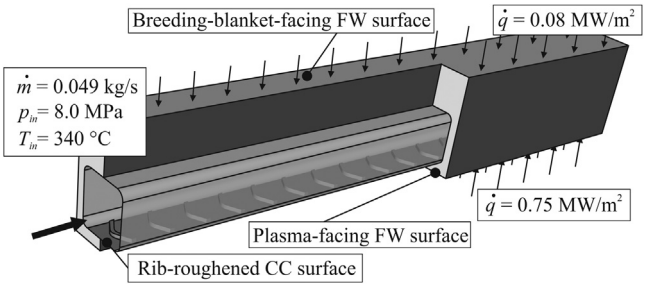

Fig. 1. Computational domain of the First Wall cooling channel.

Table 1
Geometry parameters.

Rib-height and width e	1 mm
Rib-pitch p	10 mm
Hydraulic-diameter D_h	15.668 mm (attached) 15.324 mm (detached)

be small compared to the benefits of the enhanced heat transfer, e.g. increased component life time. Flow and temperature fields of attached rib-arrays were investigated extensively for decades [3–5]. The applicability of rib-roughened CC for helium-gas cooled FW applications and their prospects of success in efficiency and effectiveness were depicted by Ruck and Arbeiter 2016 [1], Arbeiter et al., 2016 [6] and Chen and Arbeiter 2015 [7].

The objectives of the present study were to evaluate the pressure drop, heat transfer coefficients and the efficiency of FW CC structured by several rib-array configurations. The presented CC designs were studied for the 'integrated' FW concept, but can be adopted to the 'de-coupled' FW concept.

2. Numerical methods

2.1. Computational domain

Flow and conjugated heat transfer were computed for an unscaled section of the FW of DEMO including the solid structure and fluid domain as shown in Fig. 1. The FW total thickness was 30 mm and the thickness of the plasma-facing side wall was 3 mm. The channel cross section was 15 mm × 15 mm. Depending on the rib-configuration, four or two channel corners were round-edged with 2 mm radius as displayed in Fig. 2. The geometry parameters of the CC are given in Table 1.

The plasma-facing CC surface was structured by (A) attached rib-arrays and (D) detached rib-arrays of 18 centrally positioned, (T) transversally oriented ribs or (V) upstream directed 60° V-shaped ribs with different rib cross sections ((1) square, (2) 2 mm radius round-edged front- and rear-rib-surface, (3) trapezoid). For the detached rib-arrays the clearance to the channel wall was c = 0.1 mm. The length of the computational domain was 180 mm. The rib-array configurations are sketched in Fig. 2.

2.2. Simulation details and boundary conditions

Turbulent flow and heat transfer were computed by the delayed Detached-Eddy-Simulation (DDES) approach. The commercial finite-volume-method solver FLUENT V.15 [8] was used. Details of the applied algorithm and discretization schemes are described in Ruck and Arbeiter 2016 [2]. The computations were conducted for pressurized helium-gas with a mass flow rate of $\dot{m}$ = 0.049 kg/s (corresponding to a Reynolds number of Re = 1.05 × 10^5 based on the hydraulic diameter D_h), with an inlet pressure of p_{in} = 8 MPa(abs) and with an inlet temperature of T_{in} = 340 °C. Assuming ideal gas conditions the specific heat capacity c_p^{He}, the thermal conductivity k^{He} and the fluid viscosity μ^{He} were determined [9]. The baseline structural material for the FW was EUROFER steel [10] with the specific heat capacity c_p^E [11], thermal conductivity k^E [12] and a density of ρ^E = 7620 kg/m³ for the expected temperature range. Symmetry conditions were employed at the outer side, rear and front walls of the solid domain. Peak heat flux densities on the FW were assumed to be in the range from 0.5 MW/m² to 1.0 MW/m² [13] and, thus, a constant heat flux density of 0.75 MW/m² was applied on the plasma-facing FW surface. A heat flux density of 0.08 MW/m² was assumed to occur on the breeding-blanket-facing FW surface, see Fig. 1. This non-uniform heat flux distribution around the channel perimeter is characteristic for the FW and motivates the application of one-sided heat transfer enhancement [6].

The inlet flow was fully developed. The corresponding velocity profile was obtained separately by isothermal, transient DDES flow simulations in a smooth CC with identical geometrical dimensions as the structured CC. Simulations were transient with a CFL number < 1.0. Time-averaging of the results were carried out, after a computationally developed state was reached, for a time period of hundred flow-throughs over one rib-pitch-section.

The fluid mesh size for the different rib-configurations was up to 24.4 × 10^6 cells. Local grid refinement was performed in the vicinity of the ribs and within the inter-rib-spacing resulting in a focus region with maximum cells sizes of $\Delta x^+ \leq 40$ (streamswise) and $\Delta y^+ \approx \Delta z^+ \leq 25$ (span- and crosswise) and a wall-normal first spacing of $\Delta z^+ < 1$. Numerical uncertainty has been verified by the grid convergence index method as indicated by Roache 1994 [14] and recommended for CFD Studies [15].

2.3. Manufacturing concepts

The design of the structured FW CC depends on different manufacturing strategies, currently considered for the helium cooled FW. The presented design of the attached rib-arrays bases on the manufacturing strategy of fabricating the FW from two separate shells with the intersection plane at the channel symmetry plane and joining the upper and lower shell by the HIP technique [16]. The CC with the attached rib-arrays are designed for a generation of usual machining of mill cutting with cylindrical and spherical head cutters.

For generation the detached rib-arrays, ladder-like tapes of ribs can be inserted into support notches located at the CC side walls. The CC (including the support notches) can be fabricated by wire cutting electrical discharge machining [17]. The concept of inserting ladder-like tapes can be adopted for the design and fabrication of the attached rib-arrays by generating two support notches into the CC bottom. Both concepts of ladder-like tape insertion manufacturing are sketched in Fig. 3. Compared to concepts with the die sink erosion techniques for generating rib-roughened CC surfaces, a cost reduction for producing the rib-roughened CC surfaces per channel length is expected to be in the range of two orders of magnitude by the ladder-like tape insertion manufacturing. To improve the fitting and to ensure a fixation of the ladder-like rib-arrays, structural materials with a higher thermal expansion than the FW structural material can be considered for the ribs.

3. Results

3.1. Heat transfer coefficient and pressure drop

The local distributions of the heat flux densities at the rib-roughened CC surface varied along the CC. The heat transfer coefficient, evaluated with the spatially averaged coolant bulk tem-

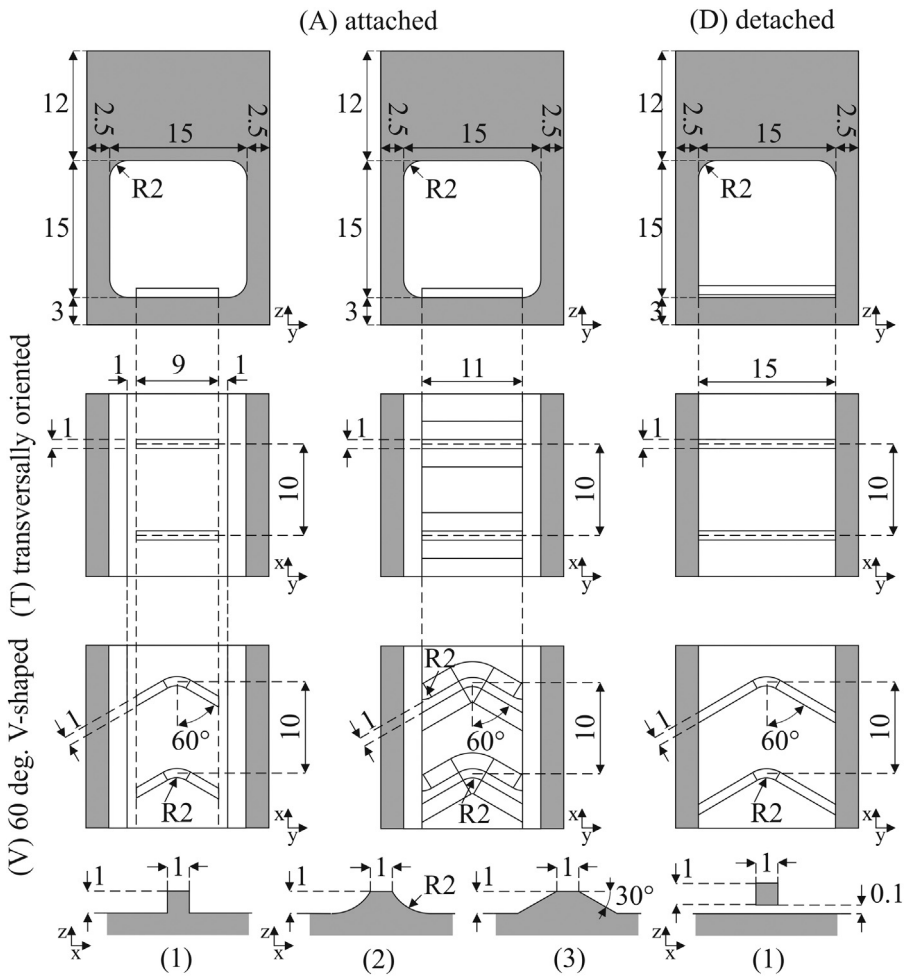

Fig. 2. Rib-array configurations of the First Wall cooling channels. All dimensions are given in mm.

perature $\bar{T}_b$, the heat flux density $\bar{q}_r$ and the wall temperature $\bar{T}_r$ over each pitch-rib-section area of the rib-roughened CC surface within the fully thermal-hydraulically developed region,

$$h_r = \bar{q}_r / \left(\bar{T}_r - \bar{T}_b\right) \quad (1)$$

and the corresponding mean axial pressure drop dp/dx along the CC are shown in Fig. 4. For the transversally oriented and V-shaped attached rib-arrays, the heat transfer coefficients were increased for different rib cross sections in the order: trapezoid, 2 mm radius round-edged front- and rear-rib-surface and square. The pressure drop was reduced for the trapezoid cross section and was in a comparable range for the remaining ones. The varying pressure drop and heat transfer coefficient were attributed to thermal-hydraulic effects caused by the different cross sections. The simulation results showed that the flow moves smoother over the rib-arrays with trapezoid cross section than over the square cross section and, thus, flow acceleration and deceleration decrease and the pressure and velocity gradients are reduced and smoothed. Furthermore, compared to the square rib cross section, the heat transfer area was reduced for the ribs with the 2 mm radius round-edged front- and rear-rib-surface and trapezoid cross section. The heat transfer area of the rib-roughened wall of the AV1 configuration was increased about 19% compared to a smooth channel geometry. The increased pressure drop of the detached rib-arrays was partly attributed to the increased form drag due to the enlarged transversal cross-sectional area and to the development of flow stagnation regions at the conjunction of the ribs and the sidewalls, accompanied by a decrease of momentum transport and pressure penalty. Effects of the gap flow and wall-jet flow beneath and behind the ribs slightly raised the pressure drop as indicated by Liou et al. [18]. Heat transfer coefficients of attached and detached ribs were in a comparable range. Therefore, it can be concluded that small gaps in the order

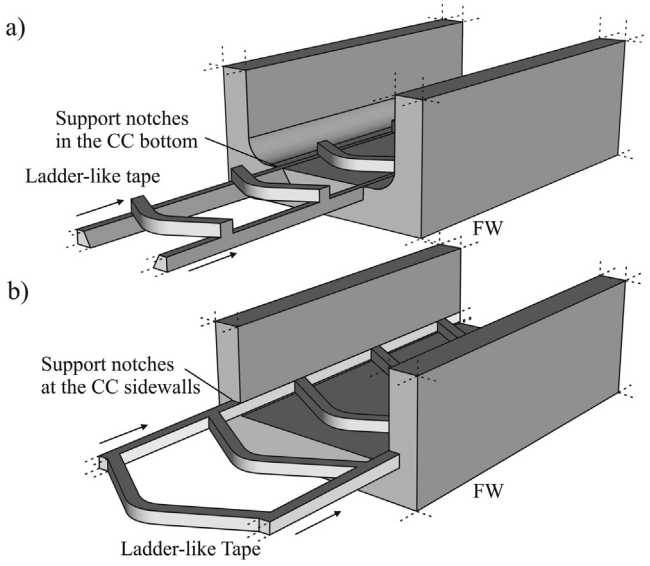

Fig. 3. Ladder-like manufacturing concepts for a) attached rib-arrays and b) detached rib-arrays.

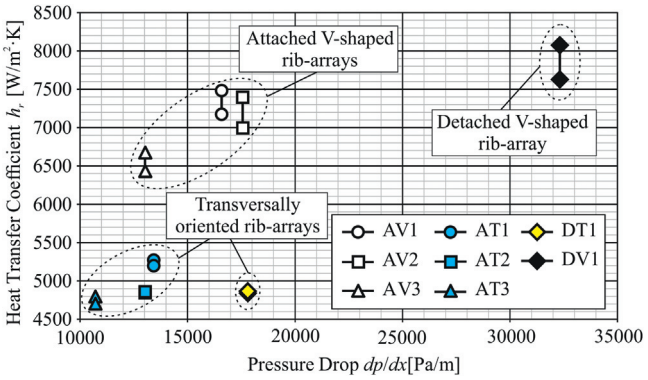

Fig. 4. Heat transfer coefficient and pressure drop within the fully thermal-hydraulically developed region.

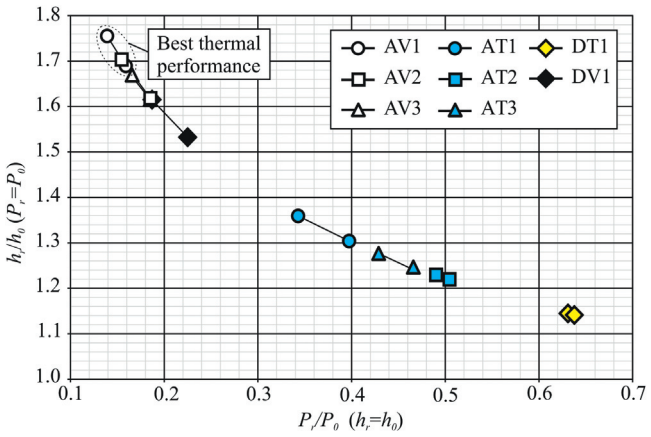

Fig. 5. Thermal performance of the investigated FW cooling channels.

of common manufacturing tolerance occurring between the rib-roughened CC surface and the ribs which are generated by the ladder-like tape insertion manufacturing will not reduce the global functionality of cooling the FW, but can raise the required pumping power when compared to fully attached ribs.

Compared to the transversally oriented rib-arrays the pressure drop and heat transfer coefficient of the V-shaped rib-arrays were increased. The V-shaped rib configuration caused stronger secondary flow structures in crosswise direction. Vertical flow velocities were up to 4 times higher than for the transversally oriented rib-arrays. Thus, the mixing between the 'hot' wall boundary layer flows and the 'cold' core flow was intensified and heat transfer enhancement at the rib-roughened CC surface and at the sidewalls of the CC was significantly increased for the V-shaped rib-arrays. However, the intensified secondary flow motion raised the pressure drop enormously. The highest heat transfer coefficients were obtained for the AV1 and the DV1 rib-array and were in the range of $h_r = 7170 - 7480\,W/m^2\,K$ and $h_r = 7620 - 8080\,W/m^2\,K$ respectively. Compared to corresponding smooth channel geometries, the heat transfer coefficient was increased about 244% and 263% for the given boundary conditions. The heat transfer coefficients of the transversally oriented rib-arrays were in the range of $h_r = 4700 - 5270\,W/m^2\,K$.

3.2. Thermal performance

The thermal performance can be evaluated by comparing the heat transfer coefficient of the rib-roughened CC (h_r) and the heat transfer coefficient of a smooth CC (h_0) with equal thermophysical properties φ and characteristic CC lengths l_{ch} for the constraint of constant pumping power $P_r/P_0 = f_r \cdot \dot{m}_r^3 \cdot C(\varphi, l_{ch}, \ldots)/f_0 \cdot \dot{m}_0^3 \cdot C(\varphi, l_{ch}, \ldots) = 1$, with the pumping power P_r and P_0, the friction factor f_r and f_0, the mass flow rate $\dot{m}_r$ and $\dot{m}_0$ and the constant C for the rib-roughened and smooth CC respectively, as recommended by Liou and Hwang [19]. The friction factor is derived from the pressure drop $f_r = 0.5 \cdot dp/dx \cdot \rho \cdot D_h \cdot A^2 \cdot \dot{m}_r^{-2}$. The mass flow rate $\dot{m}_0$ and the heat transfer coefficient h_0 of the smooth CC can be calculated iteratively from the friction factor and Nusselt number correlation of Petukhov and Gnielinski respectively [20]. Here h_0 is the heat transfer coefficient which is provided by a smooth CC for the pumping power of the rib-roughened CC and the ratio h_r/h_0 ($Pr = P_0$) specify theheat transfer performance. On the other side, the thermal performance can be evaluated by comparing the required pumping power of the rib-roughened CC P_r and a smooth CC P_0 for the constraint of equivalent heat transfer performance, $h_r = h_0$. Applying an analogous calculation procedure the ratio P_r/P_0 ($h_r = h_0$) can be evolved. Here P_0 is the pumping power for the smooth CC which is required to provide the heat transfer rate of the rib-roughened CC. Therefore, the ratio P_r/P_0 ($h_r = h_0$) specifies the reduced or increased pumping power for an equivalent heat transfer performance. The ratio h_r/h_0 ($P_r = P_0$) is plotted against the ratio P_r/P_0 ($h_r = h_0$) for the different rib-arrays in Fig. 5. All investigated rib-arrays showed increased thermal performance, h_r/h_0 ($P_r = P_0$) > 1 and P_r/P_0 ($h_r = h_0$) < 1. Best efficiency was obtained for the AV1 rib-array (highest h_r/h_0 ($P_r = P_0$) and smallest P_r/P_0 ($h_r = h_0$)). Compared to smooth channel flows, only 14–16% of the pumping power is required to obtain the equivalent heat transfer performance or, from another point of view, the heat transfer coefficient can be increased by 168–172% for constant pumping power.

4. Conclusion

The applicability of different rib-arrays for increasing the cooling performance of the helium-gas cooled First Wall cooling channels were analyzed. Based on results of Detached Eddy Simulations, it was shown that structuring the thermally highly loaded cooling channel surfaces with optimized rib-arrays provides an efficient heat transfer and increases the cooling performance which yields reduced structural material temperatures. The main findings are summarized as follows:

(1) Cost-effective manufacturing concepts for generating rib-roughened First Wall cooling channels by the insertion of ladder-like tapes were introduced. (2) The highest heat transfer coefficients and pressure drops were caused by the detached V-shaped rib-array. (3) In general, the V-shaped rib-arrays provided the highest efficiency. (4) The best thermal performance was obtained for the attached V-shaped rib-array with square rib cross section. Compared to smooth channel flows, only 14–16% of the pumping power is required to obtain the equivalent heat transfer performance.

Acknowledgment

This work has been carried out within the framework of the EUROfusion Consortium and has received funding from the Euratom research and training programme 2014–2018 under grant agreement No 633053. The views and opinions expressed herein do not necessarily reflect those of the European Commission.

References

[1] S. Ruck, F. Arbeiter, Thermohydraulics of rib-roughened helium gas running cooling channels for first wall applications, Fusion Eng. Des. 109–111 (A) (2016) 1035–1040.

[2] S. Ruck, F. Arbeiter, Effects of rib-Configuration on the thermal-hydraulics of one-sided heated and rib-roughened cooling channels, HEFAT 12th international conference on heat transfer, Fluid Mech. Thermodyn. (2016) 407–412.
[3] G. Rau, M. Cakan, D. Moeller, T. Arts, The effect of periodic ribs on the local aerodynamic and heat transfer performance of a straight cooling channel, J. Turbomach. 120 (1998) 368–375.
[4] J.C. Han, Heat transfer and friction characteristics in rectangular channels with rib turbulators, J. Heat Transf. 110 (1988) 321–328.
[5] J.C. Han, Y.M. Zhang, C.P. Lee, Augmented heat transfer in square channels with parallel crossed, and V-shaped angled ribs, J. Heat Transf. 113 (1991) 590–596.
[6] F. Arbeiter, C. Bachmann, Y. Chen, M. Ilić, F. Schwab, B. Sieglin, R. Wenninger, Thermal-hydraulics of helium cooled First Wall channels and scoping investigations on performance improvement by application of ribs and mixing devices, Fusion Eng. Des. 109–111 (B) (2016) 1123–1129.
[7] Y. Chen, F. Arbeiter, Optimization of channel for helium cooled DEMO first wall by application of one-sided V-shape ribs, Fusion Eng. Des. 98–99 (2015) 1442–1447.
[8] ANSYS Fluent Theory Guide, Release 15.0 (2013).
[9] VDI, Heat Atlas, 2nd ed., Springer-Verlag, Berlin Heidelberg, 2010.
[10] T.R. Barrett, G. Ellwood, G. Pérez, M. Kovari, M. Fursdon, F. Domptail, S. Kirk, S.C. McIntosh, S. Roberts, S. Zheng, L.V. Boccaccini, J.-H. You, C. Bachmann, J. Reiser, M. Rieth, E. Visca, G. Mazzone, F. Arbeiter, P.K. Domalapally, Progress in the engineering design and assessment of the european DEMO first wall and divertor plasma facing components, Fusion Eng. Des. (2016), http://dx.doi.org/10.1016/j.fusengdes.2016.01.052.
[11] K. Mergia, N. Boukos, Structural, thermal, electrical and magnetic properties of Eurofer 97 steel, J. Nucl. Mater. 373 (1) (2008) 1–8.
[12] CEA. DEN-SAC Appendix A –Material Design Limit Data A3. S18E Eurofer Steel (2004).
[13] R. Wenninger, R. Kemp, F. Maviglia, H. Zohm, R. Albanese, R. Ambrosino, F. Arbeiter, J. Aubert, C. Bachmann, W. Biel, E. Fable, G. Federici, J. Garcia, A. Loarte, Y. Martin, T. Pütterich, C. Reux, B. Sieglin, P. Vincenzi, DEMO exhaust challenges beyond ITER, in: Proceedings 42nd EPS Conference on Plasma Physics, Lisbon, Portugal, 2015.
[14] P.J. Roache, Perspective a method for uniform reporting of grid refinement studies, J. Fluids Eng. 116 (3) (1994) 405–413.
[15] Procedure for estimation and reporting of uncertainty due to discretization in CFD applications, J. Fluids Eng. 130 (7) (2008).
[16] H. Neuberger, A. von der Weth, J. Rey, KIT induced activities to support fabrication, assembly and qualification of technology for the HCPB-TBM, Fusion Eng. Des. 86 (9–11) (2011) 2039–2042.
[17] H. Neuberger, J. Rey, A. von der Weth, F. Hernandez, T. Martin, M. Zmitko, A. Felde, R. Niewöhner, F. Krüger, Overview on ITER and DEMO blanket fabrication activities of the KIT INR and related frameworks, Fusion Eng. Des. 96-97 (2015) 315–318.
[18] T.-M. Liou, W.-B. Wang, Y.-J. Chang, Holographic interferometry stud of spatially periodic heat transfer in a channel with ribs detached from one wall, J. Heat Transf. 117 (1995) 32–39.
[19] T.-M. Liou, J.-J. Hwang, Developing heat transfer and friction in a ribbed rectangular duct with flow separation at inlet, J. Heat Transf. 114 (1992) 565–573.
[20] F.P. Incropera, D.P. DeWitt, Fundamentals of Heat and Mass Transfer, 6th ed., Wiley, 2007.